

# Probing few-body nuclear dynamics via $^3\text{H}$ and $^3\text{He}$ ( $e, e'p$ )pn cross-section measurements

R. Cruz-Torres,<sup>1,\*</sup> D. Nguyen,<sup>1,2,\*</sup> F. Hauenstein,<sup>3</sup> A. Schmidt,<sup>1</sup> S. Li,<sup>4</sup> D. Abrams,<sup>5</sup> H. Albataineh,<sup>6</sup> S. Alsalmi,<sup>7</sup> D. Androic,<sup>8</sup> K. Aniol,<sup>9</sup> W. Armstrong,<sup>10</sup> J. Arrington,<sup>10</sup> H. Atac,<sup>11</sup> T. Averett,<sup>12</sup> C. Ayerbe Gayoso,<sup>12</sup> X. Bai,<sup>5</sup> J. Bane,<sup>13</sup> S. Barcus,<sup>12</sup> A. Beck,<sup>1</sup> V. Bellini,<sup>14</sup> F. Benmokhtar,<sup>15</sup> H. Bhatt,<sup>16</sup> D. Bhetuwal,<sup>16</sup> D. Biswas,<sup>17</sup> D. Blyth,<sup>10</sup> W. Boeglin,<sup>18</sup> D. Bulumulla,<sup>3</sup> A. Camsonne,<sup>19</sup> J. Castellanos,<sup>18</sup> J-P. Chen,<sup>19</sup> E. O. Cohen,<sup>20</sup> S. Covrig,<sup>19</sup> K. Craycraft,<sup>13</sup> B. Dongwi,<sup>17</sup> M. Duer,<sup>20</sup> B. Duran,<sup>11</sup> D. Dutta,<sup>16</sup> E. Fuchey,<sup>21</sup> C. Gal,<sup>5</sup> T. N. Gautam,<sup>17</sup> S. Gilad,<sup>1</sup> K. Gnanvo,<sup>5</sup> T. Gogami,<sup>22</sup> J. Golak,<sup>23</sup> J. Gomez,<sup>19</sup> C. Gu,<sup>5</sup> A. Habarakada,<sup>17</sup> T. Hague,<sup>7</sup> O. Hansen,<sup>19</sup> M. Hattawy,<sup>10</sup> O. Hen,<sup>1,†</sup> D. W. Higinbotham,<sup>19</sup> E. Hughes,<sup>24</sup> C. Hyde,<sup>3</sup> H. Ibrahim,<sup>25</sup> S. Jian,<sup>5</sup> S. Joosten,<sup>11</sup> H. Kamada,<sup>26</sup> A. Karki,<sup>16</sup> B. Karki,<sup>27</sup> A. T. Katramatou,<sup>7</sup> C. Keppel,<sup>19</sup> M. Khachatryan,<sup>3</sup> V. Khachatryan,<sup>28</sup> A. Khanal,<sup>18</sup> D. King,<sup>29</sup> P. King,<sup>27</sup> I. Korover,<sup>30</sup> T. Kutz,<sup>28</sup> N. Lashley-Colthirst,<sup>17</sup> G. Laskaris,<sup>1</sup> W. Li,<sup>31</sup> H. Liu,<sup>32</sup> N. Liyanage,<sup>5</sup> P. Markowitz,<sup>18</sup> R. E. McClellan,<sup>19</sup> D. Meekins,<sup>19</sup> S. Mey-Tal Beck,<sup>1</sup> Z-E. Meziani,<sup>10,11</sup> R. Michaels,<sup>19</sup> M. Mihovilović,<sup>33,34,35</sup> V. Nelyubin,<sup>5</sup> N. Nuruzzaman,<sup>17</sup> M. Nycz,<sup>7</sup> R. Obrecht,<sup>21</sup> M. Olson,<sup>36</sup> L. Ou,<sup>1</sup> V. Owen,<sup>12</sup> B. Pandey,<sup>17</sup> V. Pandey,<sup>37</sup> A. Papadopoulos,<sup>1</sup> S. Park,<sup>28</sup> M. Patsyuk,<sup>1</sup> S. Paul,<sup>12</sup> G. G. Petratos,<sup>7</sup> E. Piasetzky,<sup>20</sup> R. Pomatsalyuk,<sup>38</sup> S. Premathilake,<sup>5</sup> A. J. R. Puckett,<sup>21</sup> V. Punjabi,<sup>39</sup> R. Ransome,<sup>40</sup> M. N. H. Rashad,<sup>3</sup> P. E. Reimer,<sup>10</sup> S. Riordan,<sup>10</sup> J. Roche,<sup>27</sup> M. Sargsian,<sup>18</sup> N. Santiesteban,<sup>4</sup> B. Sawatzky,<sup>19</sup> E. P. Segarra,<sup>1</sup> B. Schmookler,<sup>1</sup> A. Shahinyan,<sup>41</sup> S. Širca,<sup>33,42</sup> R. Skibiński,<sup>23</sup> N. Sparveris,<sup>11</sup> T. Su,<sup>7</sup> R. Suleiman,<sup>19</sup> H. Szumila-Vance,<sup>19</sup> A. S. Tadepalli,<sup>40</sup> L. Tang,<sup>19</sup> W. Tireman,<sup>43</sup> K. Topolnicki,<sup>23</sup> F. Tortorici,<sup>14</sup> G. Urciuoli,<sup>44</sup> L.B. Weinstein,<sup>3</sup> H. Witała,<sup>23</sup> B. Wojtsekhowski,<sup>19</sup> S. Wood,<sup>19</sup> Z. H. Ye,<sup>10</sup> Z. Y. Ye,<sup>45</sup> and J. Zhang<sup>28</sup>

(Jefferson Lab Hall A Tritium Collaboration)

<sup>1</sup>*Massachusetts Institute of Technology, Cambridge, MA*

<sup>2</sup>*University of Education, Hue University, Hue City, Vietnam*

<sup>3</sup>*Old Dominion University, Norfolk, VA*

<sup>4</sup>*University of New Hampshire, Durham, NH*

<sup>5</sup>*University of Virginia, Charlottesville, VA*

<sup>6</sup>*Texas A & M University, Kingsville, TX*

<sup>7</sup>*Kent State University, Kent, OH*

<sup>8</sup>*University of Zagreb, Zagreb, Croatia*

<sup>9</sup>*California State University, Los Angeles, CA*

<sup>10</sup>*Physics Division, Argonne National Laboratory, Lemont, IL*

<sup>11</sup>*Temple University, Philadelphia, PA*

<sup>12</sup>*The College of William and Mary, Williamsburg, VA*

<sup>13</sup>*University of Tennessee, Knoxville, TN*

<sup>14</sup>*INFN Sezione di Catania, Italy*

<sup>15</sup>*Duquesne University, Pittsburgh, PA*

<sup>16</sup>*Mississippi State University, Miss. State, MS*

<sup>17</sup>*Hampton University, Hampton, VA*

<sup>18</sup>*Florida International University, Miami, FL*

<sup>19</sup>*Jefferson Lab, Newport News, VA*

<sup>20</sup>*School of Physics and Astronomy, Tel Aviv University, Tel Aviv 69978, Israel*

<sup>21</sup>*University of Connecticut, Storrs, CT*

<sup>22</sup>*Tohoku University, Sendai, Japan*

<sup>23</sup>*M. Smoluchowski Institute of Physics, Jagiellonian University, PL-30348 Kraków, Poland*

<sup>24</sup>*Columbia University, New York, NY*

<sup>25</sup>*Cairo University, Cairo, Egypt*

<sup>26</sup>*Department of Physics, Faculty of Engineering,*

*Kyushu Institute of Technology, Kitakyushu 804-8550, Japan*

<sup>27</sup>*Ohio University, Athens, OH*

<sup>28</sup>*Stony Brook, State University of New York, NY*

<sup>29</sup>*Syracuse University, Syracuse, NY*

<sup>30</sup>*Nuclear Research Center -Negev, Beer-Sheva, Israel*

<sup>31</sup>*University of Regina, Regina, SK, Canada*

<sup>32</sup>*Columbia University, New York, NY*

<sup>33</sup>*University of Ljubljana, Ljubljana, Slovenia*

<sup>34</sup>*Faculty of Mathematics and Physics, Jožef Stefan Institute, Ljubljana, Slovenia*

<sup>35</sup>*Institut für Kernphysik, Johannes Gutenberg-Universität Mainz, DE-55128 Mainz, Germany*

<sup>36</sup>*Saint Norbert College, De Pere, WI*

<sup>37</sup>*Department of Physics, University of Florida, Gainesville, FL*

<sup>38</sup>*Institute of Physics and Technology, Kharkov, Ukraine*

<sup>39</sup>*Norfolk State University, Norfolk, VA*

<sup>40</sup>*Rutgers University, New Brunswick, NJ*

<sup>41</sup>*Yerevan Physics Institute, Yerevan, Armenia*

<sup>42</sup>*Faculty of Mathematics and Physics, Jožef Stefan Institute, Ljubljana, Slovenia*

<sup>43</sup>*Northern Michigan University, Marquette, MI*

<sup>44</sup>*INFN, Rome, Italy*

<sup>45</sup>*University of Illinois-Chicago, IL*

(Dated: today)

We report the first measurement of the  $(e, e'p)$  three-body breakup reaction cross sections in Helium-3 ( $^3\text{He}$ ) and Tritium ( $^3\text{H}$ ) at large momentum transfer ( $\langle Q^2 \rangle \approx 1.9 \text{ (GeV/c)}^2$ ) and  $x_B > 1$  kinematics, covering a missing momentum range of  $40 \leq p_{\text{miss}} \leq 500 \text{ MeV/c}$ . The measured cross sections are compared with different plane-wave impulse approximation (PWIA) calculations, as well as a generalized Eikonal-Approximation-based calculation that includes the final-state interaction (FSI) of the struck nucleon. Overall good agreement is observed between data and Faddeev-formulation-based PWIA calculations for the full  $p_{\text{miss}}$  range for  $^3\text{H}$  and for  $150 \leq p_{\text{miss}} \leq 350 \text{ MeV/c}$  for  $^3\text{He}$ . This is a significant improvement over previous studies at lower  $Q^2$  and  $x_B \sim 1$  kinematics where PWIA calculations differ from the data by up to 400%. For  $p_{\text{miss}} \geq 250 \text{ MeV/c}$ , the inclusion of FSI makes the calculation agree with the data to within about 10%. For both nuclei PWIA calculations that are based on off-shell electron-nucleon cross-sections and exact three-body spectral functions overestimate the cross-section by about 60% but well reproduce its  $p_{\text{miss}}$  dependence. These data are a crucial benchmark for few-body nuclear theory and are an essential test of theoretical calculations used in the study of heavier nuclear systems.

Understanding the structure and properties of nuclear systems is a formidable challenge with implications ranging from the formation of elements in the universe to their application in laboratory measurements of fundamental interactions. Due to the complexity of the strong nuclear interaction, nuclear systems are often described using effective models that are based on various levels of approximations. Testing and benchmarking such approximations is a high priority of modern nuclear physics research.

The three nucleon system plays a special role in this endeavor as its ground state is complex but still exactly calculable. Therefore studies of Helium-3 ( $^3\text{He}$ ) and Tritium ( $^3\text{H}$ ) nuclei, especially using electron-scattering reactions, serve as a precision test of modern nuclear theory [1]. While there is a lot of electron scattering data on  $^3\text{He}$  [2–10],  $^3\text{H}$  data are very sparse due to the safety limitations associated with placing a radioactive gas target in a high-current electron beam.

In the early 60's the Stanford Linear Accelerator Center (SLAC) measured  $^3\text{He}$  and  $^3\text{H}$   $(e, e')$  and  $(e, e'p)$  to extract their elastic form factors and to test theoretical models of the three-nucleon wave functions [11–14]. In the late 80's MIT-Bates and Saclay extended the  $(e, e')$  measurements to higher momentum transfer with improved accuracy [15–20]. However, despite significant theoretical advances, no new electron scattering data on  $^3\text{H}$  were published in over 30 years.

Here we study the distributions of protons in  $^3\text{He}$  and in  $^3\text{H}$  using high-energy quasi-elastic (QE) electron scattering. The simultaneous measurement of both  $^3\text{He}$  and  $^3\text{H}(e, e'p)$  cross sections places stringent constraints on the possible contribution of non-QE reaction mechanisms to our measurement, thereby increasing its sensitivity to the properties of the  $^3\text{He}$  and  $^3\text{H}$  ground-states.

This work follows a recent extraction of the  $^3\text{He}(e, e'p)$  to  $^3\text{H}(e, e'p)$  cross-section ratio [21]. The measured cross-section ratio was expected to be largely insensitive to non-QE reaction mechanisms and thereby to test calculations of the ratio of proton momentum distributions in the measured nuclei. The results agreed with theoretical calculations for reconstructed initial proton momenta below 250 MeV/c. However, the theoretical calculations underpredicted the measured ratio by 20% - 50% for momenta between 250 and 550 MeV/c. Therefore, the individual  $^3\text{He}$  and  $^3\text{H}(e, e'p)$  cross-sections were needed to understand whether the observed disagreement arose from contributions of non-QE reaction mechanisms that do not cancel in the measured ratio or due to deficiencies in either nucleus wave function calculations. The results of this study are reported herein.

We find that our cross sections are better described by PWIA calculations than previous works, that  $^3\text{H}$  is better described than  $^3\text{He}$ , and that including leading nucleon rescattering further improved the agreement with theory. The remaining difference between data and theory is opposite for  $^3\text{He}$  and  $^3\text{H}$ , leading to the previously observed large discrepancy in  $^3\text{He}/^3\text{H}$  cross-section ratio that might be explained by charge exchange processes.

The experiment took place in 2018 at Hall A of the

\* Equal Contribution

† Contact Author hen@mit.edu

Thomas Jefferson National Accelerator Facility (JLab). It used the two high-resolution spectrometers (HRSs) [22] and a 20  $\mu\text{A}$  electron beam at 4.326 GeV incident on one of four identical 25-cm long gas target cells filled with Hydrogen ( $70.8 \pm 0.4 \text{ mg/cm}^2$ ), Deuterium ( $142.2 \pm 0.8 \text{ mg/cm}^2$ ), Helium-3 ( $53.4 \pm 0.6 \text{ mg/cm}^2$ ), and Tritium ( $85.1 \pm 0.8 \text{ mg/cm}^2$ ) [23].

Each HRS consisted of three quadrupole magnets for focusing and one dipole magnet for momentum analysis [22, 24]. These magnets were followed by a detector package, slightly updated with respect to the one in Ref. [22], consisting of a pair of vertical drift chambers used for tracking, and two scintillation counter planes that provided timing and trigger signals. A  $\text{CO}_2$  Cherenkov detector placed between the scintillators and a lead-glass calorimeter placed after them were used for particle identification.

Scattered electrons were detected in the left-HRS, positioned at central momentum and angle of  $\vec{p}_e' = 3.543 \text{ GeV/c}$  and  $\theta_e = 20.88^\circ$ , giving a central four-momentum transfer  $Q^2 = \vec{q}^2 - \omega^2 = 2.0 \text{ (GeV/c)}^2$  (where the momentum transfer is  $\vec{q} = \vec{p}_e - \vec{p}_e'$ ), energy transfer  $\omega = 0.78 \text{ GeV}$ , and  $x_B \equiv \frac{Q^2}{2m_p\omega} = 1.4$  (where  $m_p$  is the proton mass). Knocked-out protons were detected in the right-HRS at two central kinematical settings of  $(\theta_p, p_p) = (48.82^\circ, 1.481 \text{ GeV/c})$ , and  $(58.50^\circ, 1.246 \text{ GeV/c})$  corresponding to low- $p_{\text{miss}}$  ( $40 \leq p_{\text{miss}} \leq 250 \text{ MeV/c}$ ) and high- $p_{\text{miss}}$  ( $250 \leq p_{\text{miss}} \leq 500 \text{ MeV/c}$ ), respectively, where  $\vec{p}_{\text{miss}} = \vec{p}_p - \vec{q}$ . The exact electron kinematics for each  $p_{\text{miss}}$  bin varied within the spectrometer acceptance, see supplementary materials Tables III-VI for details.

In the Plane-Wave Impulse Approximation (PWIA) for QE scattering, where a single exchanged photon is absorbed on a single proton and the knocked-out proton does not re-interact as it leaves the nucleus, the missing momentum and energy equal the initial momentum and separation energy of the knocked-out nucleon:  $\vec{p}_i = \vec{p}_{\text{miss}}$ ,  $E_i = E_{\text{miss}}$ , where  $E_{\text{miss}} = \omega - T_p - T_{A-1}$ ,  $T_{A-1} = (\omega + m_A - E_p) - \sqrt{(\omega + m_A - E_p)^2 - |\vec{p}_{\text{miss}}|^2}$  is the reconstructed kinetic energy of the residual  $A-1$  system.  $T_p$  and  $E_p$  are the measured kinetic and total energies of the outgoing proton.

Non-QE reaction mechanisms that lead to the same measured final state also contribute to the cross section, complicating this simple picture. Such mechanisms include rescattering of the struck nucleon (final-state interactions or FSI), meson-exchange currents (MEC), and exciting isobar configurations (IC). In addition, relativistic effects can be significant [25–27].

The kinematics of our measurement were chosen to reduce contributions from such non-QE reaction mechanisms. For high- $Q^2$  reactions, the effects of FSI were shown to be reduced by choosing kinematics where the angle between  $\vec{p}_{\text{recoil}} = -\vec{p}_{\text{miss}}$  and  $\vec{q}$  is  $\theta_{rq} \lesssim 40^\circ$ ,

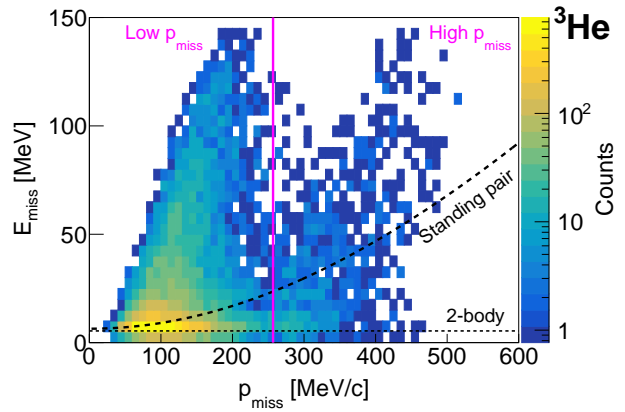


FIG. 1. The number of  ${}^3\text{He}(e, e'p)$  events as a function of  $E_{\text{miss}}$  vs  $p_{\text{miss}}$ . The solid purple line separates the high- and low- $p_{\text{miss}}$  kinematics. The dashed horizontal line labeled ‘2-body’ marks the 5-MeV two-body breakup peak and the dashed line labeled ‘Standing pair’ shows the expected  $E_{\text{miss}}-p_{\text{miss}}$  correlation for scattering off a standing SRC pair.

which also corresponds to  $x_B \geq 1$  [28–34]. Additionally MEC and IC were shown to be suppressed for  $Q^2 > 1.5 \text{ (GeV/c)}^2$  and  $x_B > 1$  [29, 35].

The raw data analysis follows that previously reported in Ref. [21] for the  ${}^3\text{He}/{}^3\text{H}(e, e'p)$  cross-section ratio extraction. We selected electrons by requiring that the particle deposits more than half of its energy in the calorimeter:  $E_{\text{cal}}/|\vec{p}| > 0.5$ . We selected  $(e, e'p)$  coincidence events by placing  $\pm 3\sigma$  cuts around the relative electron and proton event times and the relative electron and proton reconstructed target vertices (corresponding to a  $\pm 1.2 \text{ cm}$  cut). Due to the low experimental luminosity, the random coincidence event rate was negligible. We discarded a small number of runs with anomalous event rates.

Measured electrons were required to originate within the central  $\pm 9 \text{ cm}$  of the gas target to exclude events originating from the target walls. By measuring scattering from an empty-cell-like target we determined that the target cell wall contribution to the measured  $(e, e'p)$  event yield was negligible ( $\ll 1\%$ ).

To avoid the acceptance edges of the spectrometer, we only analyzed events that were detected within  $\pm 4\%$  of the central spectrometer momentum, and  $\pm 27.5 \text{ mrad}$  in in-plane angle and  $\pm 55.0 \text{ mrad}$  in out-of-plane angle relative to the center of the spectrometer acceptance. We further restricted the measurement phase-space by requiring  $\theta_{rq} < 37.5^\circ$  to minimize the effect of FSI and, in the high- $p_{\text{miss}}$  kinematics,  $x_B > 1.3$  to further suppress non-QE events.

The spectrometers were calibrated using sieve slit measurements to define scattering angles and by measuring the kinematically over-constrained exclusive  ${}^1\text{H}(e, e'p)$  and  ${}^2\text{H}(e, e'p)n$  reactions. The  ${}^1\text{H}(e, e'p)$  reaction  $p_{\text{miss}}$  resolution was better than  $9 \text{ MeV/c}$ . We veri-

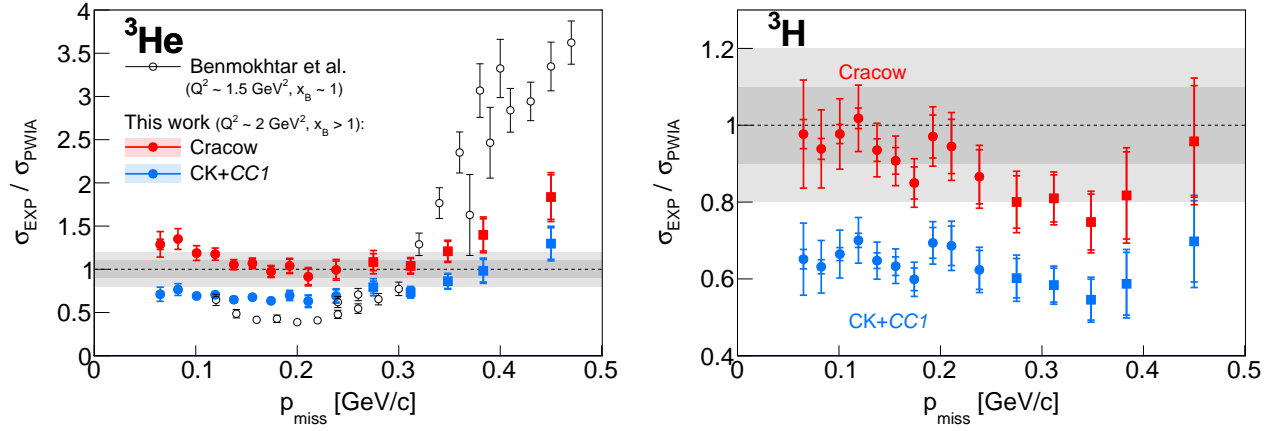


FIG. 2. The ratio of the experimental cross section to different PWIA calculations plotted versus  $p_{miss}$  for  ${}^3\text{He}(e, e'p)$  (left) and  ${}^3\text{H}(e, e'p)$  (right). Red markers show the ratio to the Cracow calculation while blue markers show the Ciofi-Kaptari spectral-function-based calculations (CK+CC1) (see text for details). Circles and squares mark low- and high- $p_{miss}$  kinematics respectively. Open symbols show the  ${}^3\text{He}(e, e'p)$  data of Ref. [3], taken at lower  $Q^2$  and  $x \sim 1$  kinematics, compared with the calculations of Ref. [32, 36–38]. The shaded regions show 10% and 20% agreement intervals.

fied the absolute luminosity normalization by comparing the measured elastic  ${}^1\text{H}(e, e')$  yield to a parametrization of the world data [39]. We also found excellent agreement between the elastic  ${}^1\text{H}(e, e'p)$  and  ${}^1\text{H}(e, e')$  rates, confirming that the coincidence trigger performed efficiently.

One significant difference between  ${}^3\text{He}(e, e'p)$  and  ${}^3\text{H}(e, e'p)$  stems from their possible final states. The  ${}^3\text{H}(e, e'p)$  reaction can only result in a three-body  $pnn$  continuum state, while  ${}^3\text{He}$  can breakup into either a two-body  $pd$  state or a three-body  $ppn$  continuum state. To allow for a more detailed comparison of the two nuclei we only considered three-body breakup reactions by requiring  $E_{miss} > 8$  MeV (i.e., above the  ${}^3\text{He}$  two-body breakup peak). See online supplementary materials for details.

Figure 1 shows the measured distribution of  ${}^3\text{He}(e, e'p)$  events as a function of  $E_{miss}$  and  $p_{miss}$ . The  ${}^3\text{H}$  and  ${}^3\text{He}$  distributions are similar with the exception that  ${}^3\text{He}$  has more strength at low  $E_{miss}$  due to the two-body breakup channel. At high- $p_{miss}$  ( $\gtrsim 250$  MeV/c) nucleons are expected to be predominantly in the form of high relative-momentum two-nucleon Short-Range Correlated (SRC) pairs [40–48]. Neglecting pair center-of-mass motion, the missing energy of such SRC pairs should be determined by their momentum such that  $E_{miss} \approx m_p - m_A + \sqrt{(m_A - m_d + \sqrt{p_{miss}^2 + m_p^2})^2 - p_{miss}^2}$ . This correlation is shown in Fig. 1 by the dashed line labeled ‘Standing pair’. Our kinematics are largely centered around this curve.

The cross-section was calculated from the  $(e, e'p)$  event yield in a given  $(p_{miss}, E_{miss})$  bin

as:

$$\frac{d^6\sigma(p_{miss}, E_{miss})}{dE_e dE_p d\Omega_e d\Omega_p} = \frac{Yield(p_{miss}, E_{miss})}{C \cdot t \cdot (\rho/A) \cdot b \cdot V_B \cdot C_{Rad} \cdot C_{BM}}, \quad (1)$$

where  $C$  is the total accumulated beam charge,  $t$  is the live time fraction in which the detectors are able to collect data,  $A = 3$  is the target atomic mass,  $\rho$  is the nominal areal density of the gas in the target cell, and  $b$  is a correction factor to account for changes in the target density caused by local beam heating.  $b$  was determined by measuring the beam current dependence of the inclusive event yield [23].  $V_B$  is a factor that accounts for the detection phase space and acceptance correction for the given  $(p_{miss}, E_{miss})$  bin and  $C_{Rad}$  and  $C_{BM}$  are the radiative and bin migration corrections, respectively. The  ${}^3\text{H}$  event yield was also corrected for the radioactive decay of  $2.78 \pm 0.18\%$  of the target  ${}^3\text{H}$  nuclei to  ${}^3\text{He}$  in the six months since the target was filled. See online supplementary materials for details.

We used the SIMC [49] spectrometer simulation package to simulate our experiment to calculate the  $V_B$ ,  $C_{Rad}$  and  $C_{BM}$  terms in Eq. 1, and to compare the measured cross-section with theoretical calculations. SIMC generates  $(e, e'p)$  events with the addition of radiation effects over a wide phase-space, propagates the generated events through a spectrometer model to account for acceptance and resolution effects, and then weights each accepted event by a model cross-section calculated for the original kinematics of that specific event. The weighted events are subsequently analyzed as the data and can be used to compare between the data and different model cross-section predictions.

We considered two PWIA cross-section models: (1) Faddeev-formulation-based calculations by J. Golak et al. [1, 50, 51] that either includes or excludes the con-

tinuum interaction between the two spectator nucleons (FSI<sub>23</sub>), labeled Cracow and Cracow-PW respectively and (2) a factorized calculation using the  $^3\text{He}$  spectral function of C. Ciofi degli Atti and L. P. Kaptari including FSI<sub>23</sub> [52] and the  $\sigma_{cc1}$  electron off-shell nucleon cross-section [53], labeled CK+CC1. Due to the lack of  $^3\text{H}$  proton spectral functions, we assumed isospin symmetry and used the  $^3\text{He}$  neutron spectral function for the  $^3\text{H}(e, e'p)$  simulation. In addition, as the Cracow calculation used the CD-Bonn nucleon-nucleon potential [54] and CK used AV18 [55]. To make consistent comparisons within this work, we have chosen to rescale the CK calculation for each nucleus by the ratio of the proton momentum distribution obtained with CD-Bonn relative to that obtained with AV18 based on calculations in Ref. [56]. See online supplementary materials for details.

We corrected the  $^3\text{He}$  and  $^3\text{H}$  cross-sections for radiation and bin migration effects using SIMC and the CK+CC1 cross-section model. Due to the excellent resolution of the HRS, bin migration effects were very small. Radiation effects were also small for  $^3\text{H}$  ( $\lesssim 20\%$ ), but significant for  $^3\text{He}$  at low- $p_{\text{miss}}$  due to two-body breakup events that reconstructed to  $E_{\text{miss}} > 8$  MeV due to radiation. Since the cross section at high  $E_{\text{miss}}$  is dominated by radiative effects, we required  $E_{\text{miss}} < 50$  and 80 MeV for the low- and high- $p_{\text{miss}}$  kinematics respectively. See online supplementary materials for details.

We then integrated the two dimensional experimental and theoretical cross sections,  $\sigma(p_{\text{miss}}, E_{\text{miss}})$ , over  $E_{\text{miss}}$  to get the cross sections as a function of  $p_{\text{miss}}$ .

To facilitate comparison with future theoretical calculations, we bin-centered the resulting cross-sections, using the ratio of the point theoretical cross section to the acceptance-averaged theoretical cross section. We calculated the point theoretical cross section by summing the cross section evaluated at the central ( $\langle Q^2 \rangle, \langle x_B \rangle$ ) values over the seven  $E_{\text{miss}}$ -bins for that  $p_{\text{miss}}$  as follows:

$$\sigma_{\text{point}}(p_{\text{miss}}) = \sum_{j=1}^N \sigma(\langle Q^2 \rangle^j, \langle x_B \rangle^j, p_{\text{miss}}, E_{\text{miss}}^j) \times \Delta E_{\text{miss}}^j \quad (2)$$

where  $j$  labels the  $E_{\text{miss}}$  bin and  $\Delta E_{\text{miss}}^j$  is the bin width. We used both the Cracow and CK+CC1 cross-section models for this calculation, taking their average as the correction factor and their difference as a measure its uncertainty. Future calculations can directly compare to our data by calculating the cross section at a small number of points and using Eq. 2, rather than by computationally-intensive integration over spectrometer acceptances. See online supplementary materials for details.

The point-to-point systematical uncertainties due to the event selection criteria (momentum and angular acceptances, and  $\theta_{rq}$  and  $x_B$  limits) were determined by

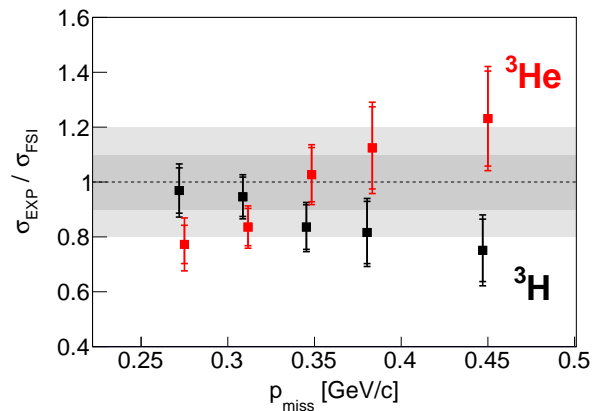


FIG. 3. The ratio of the experimental cross sections to the calculation of Sargsian that includes FSI of the leading nucleon for  $^3\text{He}$  (red squares) and  $^3\text{H}$  (black circles). The shaded regions show 10% and 20% agreement intervals.

repeating the analysis 100 times, selecting each criterion randomly within reasonable limits for each iteration. The systematic uncertainty was taken to be the standard deviation of the resulting distribution cross sections. They range from 1% to 8% and are typically much smaller than the statistical uncertainties. Additional point-to-point systematics are due to bin-migration, bin-centering and radiative corrections and range between 0.5% and 3.5%. See online supplementary Materials Table VIII and IX for details.

The overall normalization uncertainty of our measurement equals 2%, and is due to uncertainty in the target density (1.5%), beam-charge measurement run-by-run stability (1%), Tritium decay correction (0.15%), and spectrometer detection and trigger efficiencies (1%).

For completeness we also used SIMC to calculate the acceptance-averaged cross sections using both Cracow and CK+CC1 cross-section models and compared them to our measured data before any bin-centering corrections. Both models well reproduce the shape of the measured  $E_{\text{miss}}$  and  $p_{\text{miss}}$  event distributions. The ratio of the acceptance-averaged experimental to theoretical cross-section is similar to the bin-centered ratios shown here. See online Supplementary Materials Tables III-VI and Figs. 9 and 10 for details.

Fig. 2 shows the experimental, bin-centered,  $^3\text{He}$  and  $^3\text{H}$  cross-sections divided by the different PWIA calculations as a function of  $p_{\text{miss}}$  and integrated over  $E_{\text{miss}}$  from 8 to 50 or 80 MeV for the low- and high- $p_{\text{miss}}$  kinematics, respectively. For  $^3\text{H}$ , the Cracow calculation agrees with the data to about 20%. For  $^3\text{He}$ , the two agree for  $150 \leq p_{\text{miss}} \leq 350$  MeV/c but disagree by up to a factor of two for larger and lower  $p_{\text{miss}}$ . For both nuclei the CK+CC1 calculation is higher than the data by about 60%.

The most recent high- $Q^2$  measurements of the

$^3\text{He}(e, e'p)$  three-body breakup cross-sections were done at  $Q^2 = 1.5 \text{ (GeV/c)}^2$  and  $x_B = 1$  [3], near the expected maximum of struck-proton rescattering. The measured cross-sections were lower than PWIA calculations by a factor of  $\sim 2$  for  $p_{\text{miss}} < 250 \text{ MeV/c}$  and higher by a factor of  $\sim 3$  for  $400 < p_{\text{miss}} < 500 \text{ MeV/c}$  (see Fig. 2). These deviations were described by calculations which included the contribution of non-QE reaction mechanisms, primarily FSI [32, 36–38]. The large contribution of such non-QE reaction mechanisms to the measured  $(e, e'p)$  cross-sections limited their ability to constrain the nucleon distributions at high momenta. These non-QE effects are much smaller in the current measurement due to our choice of kinematics.

In order to estimate the effects of struck-proton rescattering, we also considered a cross-section calculation by M. Sargsian [57] that accounts for the FSI of the struck-nucleon using the generalized Eikonal approximation [58, 59]. This calculation does not include the continuum interaction between the two spectator nucleons, FSI<sub>23</sub>, and is therefore only applicable where those effects are small. To assess this effect we compared the available calculations with and without FSI<sub>23</sub> and found that its effects are very large at low- $p_{\text{miss}}$  but are small at  $p_{\text{miss}} > 250 \text{ MeV/c}$  (see online supplementary materials Fig. 11). We therefore use the Sargsian FSI calculations only at  $p_{\text{miss}} \geq 250 \text{ MeV/c}$ . We further verified that using this model for bin centering does not result in significantly different correction factors.

Fig. 3 shows the ratio of the experimental, bin-centered cross-section to the Sargsian FSI calculation for  $p_{\text{miss}} > 250 \text{ MeV/c}$ . The FSI calculation overall agrees with the data. The general trend of the ratio seems to be opposite for  $^3\text{He}$  and  $^3\text{H}$  with the former rising above unity while the latter decreasing below it. In an SRC-dominance model where the electron scatters primarily off nucleons in  $np$ -SRC pairs, this trend might be caused by single-charge exchange with the spectator nucleon which would increase the  $^3\text{He}(e, e'p)$  cross-section due to the spectator being a proton, but decrease the  $^3\text{H}(e, e'p)$  cross-section due to the spectator being a neutron. This hypothesis is supported by the observation that the total  $A = 3$  cross-section (i.e.  $^3\text{He} + ^3\text{H}$ ) is well reproduced by the calculation (see supplementary materials Fig. 12). Future calculations are needed to properly quantify this effect.

To conclude,  $^3\text{He}$  and  $^3\text{H}(e, e'p)$  cross-sections were measured for the first time in over 30 years. The measurement was done in high- $Q^2$  and  $x_B > 1$  kinematics covering  $40 \leq p_{\text{miss}} \leq 500 \text{ MeV/c}$ . We required that the momentum direction of the recoil nucleus be within  $37.5^\circ$  of  $\vec{q}$  to reduce the effects of leading-nucleon rescattering.

Measured cross-sections are compared with state-of-the-art PWIA and FSI cross-section calculations. The agreement between data and theory for  $^3\text{He}$  is significantly better than that of previous work at lower  $Q^2$  and  $x_B \sim 1$  kinematics. An overall good agreement is ob-

served between  $^3\text{H}$  data and theory for all  $p_{\text{miss}}$ . The same is not true for  $^3\text{He}$  at high and low  $p_{\text{miss}}$ . Including FSI of the leading nucleon in the calculation improves its agreement with the data at high- $p_{\text{miss}}$ .

These data are a crucial benchmark for few-body nuclear theory and are an essential test of theoretical calculations used in the study of heavier nuclear systems.

We acknowledge the contribution of the Jefferson-Lab target group and technical staff for design and construction of the Tritium target and their support running this experiment. We thank C. Ciofi degli Atti and L. Kaptari for the  $^3\text{He}$  spectral function calculations and M. Sargsian for the FSI calculations. We also thank M. Strikman for many valuable discussions. This work was supported by the U.S. Department of Energy (DOE) grant DE-AC05-06OR23177 under which Jefferson Science Associates, LLC, operates the Thomas Jefferson National Accelerator Facility, the U.S. National Science Foundation, the Pazi foundation, and the Israel Science Foundation. The Kent State University contribution is supported under the PHY-1714809 grant from the U.S. National Science Foundation. The University of Tennessee contribution is supported by the DE-SC0013615 grant. The work of ANL group members is supported by DOE grant DE-AC02-06CH11357. The contribution of the Cracow group was supported by the Polish National Science Centre under Grants No. 2016/22/M/ST2/00173 and No.2016/21/D/ST2/01120. The numerical calculations were partially performed on the supercomputer cluster of the JSC, Jülich, Germany. The Temple University group is supported by the DOE award DE-SC0016577.

- 
- [1] J. Golak, R. Skibiński, H. Witała, W. Glöckle, A. Nogga, and H. Kamada, *Phys. Rept.* **415**, 89 (2005), arXiv:nucl-th/0505072 [nucl-th].
  - [2] I. Sick, *Prog. Part. Nucl. Phys.* **47**, 245 (2001), arXiv:nucl-ex/0208009 [nucl-ex].
  - [3] F. Benmokhtar *et al.* (Jefferson Lab Hall A), *Phys. Rev. Lett.* **94**, 082305 (2005), arXiv:nucl-ex/0408015 [nucl-ex].
  - [4] M. M. Rvachev *et al.* (Jefferson Lab Hall A), *Phys. Rev. Lett.* **94**, 192302 (2005), arXiv:nucl-ex/0409005 [nucl-ex].
  - [5] E. Long *et al.*, *Phys. Lett.* **B797**, 134875 (2019), arXiv:1906.04075 [nucl-ex].
  - [6] M. Mihovilovic *et al.* (Jefferson Lab Hall A), *Phys. Rev. Lett.* **113**, 232505 (2014), arXiv:1409.2253 [nucl-ex].
  - [7] M. Mihovilovi *et al.* (Jefferson Lab Hall A), *Phys. Lett.* **B788**, 117 (2019), arXiv:1804.06043 [nucl-ex].
  - [8] Y. W. Zhang *et al.*, *Phys. Rev. Lett.* **115**, 172502 (2015), arXiv:1502.02636 [nucl-ex].
  - [9] A. Camsonne *et al.*, *Phys. Rev. Lett.* **119**, 162501 (2017), [Addendum: *Phys. Rev. Lett.* **119**, no.20, 209901 (2017)], arXiv:1610.07456 [nucl-ex].
  - [10] S. Riordan *et al.*, *Phys. Rev. Lett.* **105**, 262302 (2010), arXiv:1008.1738 [nucl-ex].
  - [11] H. Collard, R. Hofstadter, A. Johansson, R. Parks,



- M. Ryneveld, A. Walker, M. R. Yearian, R. B. Day, and R. T. Wagner, Phys. Rev. Lett. **11**, 132 (1963).
- [12] L. I. Schiff, H. Collard, R. Hofstadter, A. Johansson, and M. R. Yearian, Phys. Rev. Lett. **11**, 387 (1963).
- [13] A. Johansson, Phys. Rev. **136**, B1030 (1964).
- [14] T. A. GRIFFY and R. J. OAKES, Rev. Mod. Phys. **37**, 402 (1965).
- [15] K. Dow, *Proceedings, Three Body Forces in the Three Nucleon System: Washington, DC, April 24-26, 1986*, Lect. Notes Phys. **260**, 346 (1986).
- [16] D. H. Beck, *Proceedings, Three Body Forces in the Three Nucleon System: Washington, DC, April 24-26, 1986*, Lect. Notes Phys. **260**, 138 (1986).
- [17] D. Beck *et al.*, Phys. Rev. Lett. **59**, 1537 (1987).
- [18] K. Dow *et al.*, Phys. Rev. Lett. **61**, 1706 (1988).
- [19] F. P. Juster *et al.*, Phys. Rev. Lett. **55**, 2261 (1985).
- [20] A. Amroun *et al.*, Nucl. Phys. **A579**, 596 (1994).
- [21] R. Cruz-Torres *et al.* (Jefferson Lab Hall A Tritium), Phys. Lett. **B797**, 134890 (2019), arXiv:1902.06358 [nucl-ex].
- [22] J. Alcorn *et al.*, Nucl. Instrum. Meth. **A522**, 294 (2004).
- [23] S. N. Santiesteban *et al.*, Nucl. Instrum. Meth. **A940**, 351 (2019), arXiv:1811.12167 [physics.ins-det].
- [24] “In 2016, the Quadrupole magnet closest to the target (Q1) was replaced with a normal conducting quad, with similar magnetic properties.”.
- [25] J. Gao *et al.* (The Jefferson Lab Hall A Collaboration), Phys. Rev. Lett. **84**, 3265 (2000).
- [26] J. M. Udias, J. A. Caballero, E. Moya de Guerra, J. E. Amaro, and T. W. Donnelly, Phys. Rev. Lett. **83**, 5451 (1999).
- [27] R. Alvarez-Rodriguez, J. M. Udias, J. R. Vignote, E. Garrido, P. Sarriguren, E. Moya de Guerra, E. Pace, A. Kievsky, and G. Salme, *Proceedings, 21st European Conference on Few-Body Problems in Physics (EFB21): Salamanca, Castilla y Leon, Spain, August 29-September 3, 2010*, Few Body Syst. **50**, 359 (2011), arXiv:1012.3049 [nucl-th].
- [28] W. U. Boeglin *et al.* (Hall A), Phys. Rev. Lett. **107**, 262501 (2011), arXiv:1106.0275 [nucl-ex].
- [29] M. M. Sargsian, Int. J. Mod. Phys. **E10**, 405 (2001), arXiv:nucl-th/0110053 [nucl-th].
- [30] L. L. Frankfurt, M. M. Sargsian, and M. I. Strikman, Phys. Rev. C **56**, 1124 (1997), arXiv:nucl-th/9603018 [nucl-th].
- [31] S. Jeschonnek and J. W. Van Orden, Phys. Rev. C **78**, 014007 (2008), arXiv:0805.3115 [nucl-th].
- [32] J. M. Laget, Phys. Lett. **B609**, 49 (2005), arXiv:nucl-th/0407072 [nucl-th].
- [33] M. M. Sargsian, Phys. Rev. **C82**, 014612 (2010), arXiv:0910.2016 [nucl-th].
- [34] O. Hen, L. B. Weinstein, S. Gilad, and W. Boeglin, “Proton and Neutron Momentum Distributions in  $A = 3$  Asymmetric Nuclei,” (2014), arXiv:1410.4451 [nucl-ex].
- [35] M. M. Sargsian *et al.*, J. Phys. **G29**, R1 (2003), arXiv:nucl-th/0210025 [nucl-th].
- [36] C. Ciofi degli Atti and L. P. Kaptari, Phys. Rev. Lett. **95**, 052502 (2005), arXiv:nucl-th/0502045 [nucl-th].
- [37] L. Frankfurt, M. Sargsian, and M. Strikman, Int. J. Mod. Phys. A **23**, 2991 (2008), arXiv:0806.4412 [nucl-th].
- [38] M. Alvioli, C. Ciofi degli Atti, and L. P. Kaptari, Phys. Rev. **C81**, 021001 (2010), arXiv:0904.4045 [nucl-th].
- [39] E. L. Lomon, (2006), arXiv:nucl-th/0609020 [nucl-th].
- [40] O. Hen, G. A. Miller, E. Piasetzky, and L. B. Weinstein, Rev. Mod. Phys. **89**, 045002 (2017), arXiv:1611.09748 [nucl-ex].
- [41] C. Ciofi degli Atti, Phys. Rept. **590**, 1 (2015).
- [42] E. Piasetzky, M. Sargsian, L. Frankfurt, M. Strikman, and J. W. Watson, Phys. Rev. Lett. **97**, 162504 (2006).
- [43] R. Subedi *et al.*, Science **320**, 1476 (2008).
- [44] I. Korover, N. Muangma, O. Hen, *et al.*, Phys. Rev. Lett. **113**, 022501 (2014).
- [45] O. Hen *et al.*, Science **346**, 614 (2014), arXiv:1412.0138 [nucl-ex].
- [46] E. O. Cohen *et al.* (CLAS), Phys. Rev. Lett. **121**, 092501 (2018), arXiv:1805.01981 [nucl-ex].
- [47] M. Duer *et al.* (CLAS), Nature **560**, 617 (2018).
- [48] M. Duer *et al.* (CLAS Collaboration), Phys. Rev. Lett. **122**, 172502 (2019).
- [49] “SIMC,” [https://hallcweb.jlab.org/wiki/index.php/SIMC\\_Monte\\_Carlo](https://hallcweb.jlab.org/wiki/index.php/SIMC_Monte_Carlo), Accessed: 2018-10-11.
- [50] C. Carasco *et al.*, Physics Letters B **559**, 41 (2003).
- [51] J. Bermuth *et al.*, Physics Letters B **564**, 199 (2003).
- [52] C. Ciofi degli Atti and L. P. Kaptari, Phys. Rev. C **71**, 024005 (2005), arXiv:nucl-th/0407024 [nucl-th].
- [53] T. De Forest, Nucl. Phys. A **392**, 232 (1983).
- [54] R. Machleidt, Phys. Rev. **C63**, 024001 (2001), arXiv:nucl-th/0006014 [nucl-th].
- [55] R. B. Wiringa, V. G. J. Stoks, and R. Schiavilla, Phys. Rev. C **51**, 38 (1995), arXiv:nucl-th/9408016 [nucl-th].
- [56] L. E. Marcucci, F. Sammarruca, M. Viviani, and R. Machleidt, Phys. Rev. **C99**, 034003 (2019), arXiv:1809.01849 [nucl-th].
- [57] “M. Sargsian, Private communication.”.
- [58] M. M. Sargsian, T. V. Abrahamyan, M. I. Strikman, and L. L. Frankfurt, Phys. Rev. C **71**, 044614 (2005).
- [59] M. M. Sargsian, T. V. Abrahamyan, M. I. Strikman, and L. L. Frankfurt, Phys. Rev. C **71**, 044615 (2005).